An Expanded Role for the RFX Transcription Factor DAF-19, with Dual Functions in Ciliated and Nonciliated Neurons

Elizabeth A. De Stasio,*,[1] Katherine P. Mueller,*,[2] Rosemary J. Bauer,* Alexander J. Hurlburt,* Sophie A. Bice,* Sophie L. Scholtz,* Prasad Phirke,† Debora Sugiaman-Trapman,† Loraina A. Stinson,* Haili B. Olson,* Savannah L. Vogel,* Zabdiel Ek-Vazquez,* Yagmur Esemen,* Jessica Korzynski,* Kelsey Wolfe,* Bonnie N. Arbuckle,* He Zhang,* Gaelen Lombard-Knapp,* Brian P. Piasecki,* and Peter Swoboda†

*Department of Biology, Lawrence University, Appleton, Wisconsin 54911 and †Department of Biosciences and Nutrition, Karolinska Institute, 141 83 Huddinge, Sweden

ORCID IDs: 0000-0002-4966-3409 (E.A.D.S.); 0000-0001-6416-8572 (P.S.)

ABSTRACT Regulatory Factor X (RFX) transcription factors (TFs) are best known for activating genes required for ciliogenesis in both vertebrates and invertebrates. In humans, eight RFX TFs have a variety of tissue-specific functions, while in the worm *Caenorhabditis elegans*, the sole RFX gene, *daf-19*, encodes a set of nested isoforms. Null alleles of *daf-19* confer pleiotropic effects including altered development with a dauer constitutive phenotype, complete absence of cilia and ciliary proteins, and defects in synaptic protein maintenance. We sought to identify RFX/*daf-19* target genes associated with neuronal functions other than ciliogenesis using comparative transcriptome analyses at different life stages of the worm. Subsequent characterization of gene expression patterns revealed one set of genes activated in the presence of DAF-19 in ciliated sensory neurons, whose activation requires the *daf-19c* isoform, also required for ciliogenesis. A second set of genes is downregulated in the presence of DAF-19, primarily in nonsensory neurons. The human orthologs of some of these neuronal genes are associated with human diseases. We report the novel finding that *daf-19a* is directly or indirectly responsible for downregulation of these neuronal genes in *C. elegans* by characterizing a new mutation affecting the *daf-19a* isoform (*tm5562*) and not associated with ciliogenesis, but which confers synaptic and behavioral defects. Thus, we have identified a new regulatory role for RFX TFs in the nervous system. The new *daf-19* candidate target genes we have identified by transcriptomics will serve to uncover the molecular underpinnings of the pleiotropic effects that *daf-19* exerts on nervous system function.

KEYWORDS RFX transcription factor; neuronal gene expression; dauer formation; roaming behavior; aldicarb resistance

CHARACTERIZING Regulatory Factor X (RFX) transcription factor (TF) function and identifying RFX target genes are key to understanding a wide range of diseases. Problems with RFX-controlled genes are linked to impaired immune function, cancer, and ciliopathies including developmental disorders, kidney disease, and deafness. RFX TFs regulate processes including mitosis in yeasts (Garg *et al.* 2015), ciliogenesis and cilia maintenance (Choksi *et al.* 2014), adaptive immune responses (Reith and Mach 2001), innate immunity (Xie *et al.* 2013), and maintenance of terminally differentiated hair cells in the mammalian ear (Elkon *et al.* 2015). RFX target genes encode ciliary components (*e.g.*, Schafer *et al.* 2003; Jensen *et al.* 2016), phosphatases involved in carcinogenesis (Su *et al.* 2014), major histocompatibility complex genes (Meissner *et al.* 2012), and genes associated with dyslexia (Tammimies *et al.* 2016), to name a few.

RFX TFs share and are defined by a highly conserved winged helix DNA-binding domain (DBD) (Emery *et al.* 1996; Gajiwala *et al.* 2000) by which gene networks are

doi: https://doi.org/10.1534/genetics.117.300571
Manuscript received November 29, 2017; accepted for publication January 2, 2017; published Early Online January 3, 2018.
Supplemental material is available online at www.genetics.org/lookup/suppl/doi:10.1534/genetics.117.300571/-/DC1.
[1]Corresponding author: Department of Biology, Lawrence University, 711 E. Boldt Way, SPC 24, Appleton, WI 54911. E-mail: elizabeth.a.destasio@lawrence.edu
[2]Present address: Department of Biomedical Engineering and Wisconsin Institutes for Discovery, University of Wisconsin–Madison, WI 53715.

regulated in both invertebrates and vertebrates. RFX TFs evolved early in the unikont lineage, and, though well known for controlling ciliogenesis, they apparently evolved after the origin of cilia (Chu *et al.* 2010; Piasecki *et al.* 2010). Thus, they likely have an ancient function. Humans have eight RFX genes (Aftab *et al.* 2008; https://www.ncbi.nlm.nih.gov/gene/731220). RFX TFs regulate target genes via a highly conserved *cis*-acting regulatory sequence called the X-box motif (Efimenko *et al.* 2005; Laurencon *et al.* 2007; Chu *et al.* 2012). The X-box sequence has been used effectively to identify many RFX target genes (*e.g.*, Blacque *et al.* 2005; Chen *et al.* 2006; Henriksson *et al.* 2013).

Here, we describe novel functions for *daf-19*, the only RFX gene in the worm *Caenorhabditis elegans*. DAF-19 was the first RFX TF linked to the process of ciliogenesis (Swoboda *et al.* 2000; Senti and Swoboda 2008) and it was found also to regulate innate immunity (Xie *et al.* 2013). The *C. elegans daf-19* locus encodes at least four related gene products with three transcriptional start sites (Craig *et al.* 2013). Two smaller isoforms, DAF-19C and DAF-19M (Figure 1A), have a role in ciliated sensory neurons (CSNs) only. The majority of CSNs, the only ciliated cell type in the worm, are generated during embryogenesis (Jensen *et al.* 2016). *daf-19c*, expressed in all CSNs via an internal promoter (Senti and Swoboda 2008; Craig *et al.* 2013), is sufficient to drive ciliogenesis in CSNs (Senti *et al.* 2009). DAF-19C alone is also sufficient to drive continued larval development in a food-rich environment as opposed to entering the dispersive and stress-resistant dauer larval stage (Senti and Swoboda 2008). DAF-19C regulates transcription of ciliary genes via X-box motifs supported by a nearby C-box enhancer element (Burghoorn *et al.* 2012). In contrast, the *daf-19m* isoform is expressed only in IL2 and male-specific CSNs, where it regulates the transcription of genes required for male mating behaviors, including those with orthologs implicated in polycystic kidney disease (Wang *et al.* 2010). Gene regulation by DAF-19M results in cilia specialization via a DAF-19C-independent cascade of gene expression (Wang *et al.* 2010).

Roles for the larger DAF-19A/B isoforms extend into adulthood, including regulation of foraging behavior and synaptic protein maintenance (Senti and Swoboda 2008). *daf-19a* and *b* differ by one small, alternately spliced exon (Figure 1, A–C), are highly expressed in nonciliated neurons (Saito *et al.* 2013), and are also less highly expressed in the hypodermis and body wall muscle at all life stages (Senti and Swoboda 2008; Craig *et al.* 2013). Null *daf-19*(*m86*) mutant adults expressing only transgenic DAF-19C have apparently normal cilia and sensory functions, but display abnormal dwelling and roaming behaviors (Senti and Swoboda 2008), consistent with a synaptic defect in nonsensory neurons (Flavell *et al.* 2013). This defect was confirmed by pharmacological studies and a noted reduction in certain synaptic protein levels in adults. However, RNA levels of these proteins were not similarly decreased (Senti and Swoboda 2008), suggesting an indirect regulatory effect of DAF-19A/B on synaptic protein turnover. Thus, *daf-19* promotes certain neuronal functions beyond ciliogenesis at the embryonic life stage, and these pleiotropic effects can be attributed to downstream effects of different *daf-19*-regulated genes. We sought to identify new DAF-19 target genes, particularly DAF-19A target genes that function in neurons, by characterizing post-embryonic transcriptomes of *daf-19*(*m86*) null mutants and isogenic age-matched controls at the L1 larval and adult stages of development. Transcriptome approaches have previously successfully identified new RFX target genes expressed early in worm development (Chen *et al.* 2006; Phirke *et al.* 2011; Jensen *et al.* 2016) and in other organisms, including humans (*e.g.*, Nelander *et al.* 2005; Wu *et al.* 2016).

Here, for the first time, we describe target genes of DAF-19A, in addition to new target genes of DAF-19C. Further, we characterize a new *daf-19a/b* isoform-specific mutation (*tm5562*) and demonstrate that DAF-19A/B expression is directly or indirectly responsible for the downregulation of target genes in certain nonsensory neurons, while DAF-19C primarily activates genes in CSNs. We propose that the intricate interplay of DAF-19 isoforms controls the expression of different gene batteries in defined sets of neurons, and that DAF-19 impacts neuronal functions ranging from basic synaptic maintenance to neuronal outputs in development (dauer formation) and behavior (foraging and locomotion).

Materials and Methods

C. elegans strains and culture conditions

C. elegans strains (Supplemental Material, Table S1) were cultured at 20° following standard procedures (Brenner 1974) except for LU455, *daf-19*(*m86*), grown at 15° to obtain adults for behavioral assays. Gene expression studies at multiple life stages required the *daf-12*(*sa204*) allele to fully suppress the highly penetrant dauer formation constitutive (Daf-c) phenotype conferred by *daf-19*(*m86*). *him-5*(*e1490*) was used to generate males. The *daf-19*(*tm5562*) mutant was obtained from the Mitani laboratory collection and was outcrossed to wild-type N2 six times. Three primers [upstream (U), downstream (D), and poison (P)] identified the *tm5562* deletion allele during outcrossing: U5, 5′-AATGACCTTCACA CGGTGTC-3′; D5, 5′-CACACCGGGTGCTTCACCAT-3′; and P5, 5′-GCGCACAATAGGCTCCAAGC-3′. The 865-bp deletion was confirmed by sequencing PCR amplicons after outcrossing. *daf-19*(*tm5562/+*) heterozygous and associated control animals were generated by mating to a strain carrying an integrated fluorescent marker.

L1- and adult-stage worms were collected for transcriptome analysis from JT204 *daf-12*(*sa204*) and JT6924 *daf-19*(*m86*); *daf-12*(*sa204*). To collect L1-stage worms, worms were grown on agarose-containing solid egg-NGM medium for 6–7 days until a sizeable gravid adult worm population was observed. Embryos were isolated by hypochlorite treatment and grown to the threefold stage in S-Basal medium with *Escherichia coli* OP50 with gentle agitation at 20°. A second hypochlorite treatment removed hatched worms

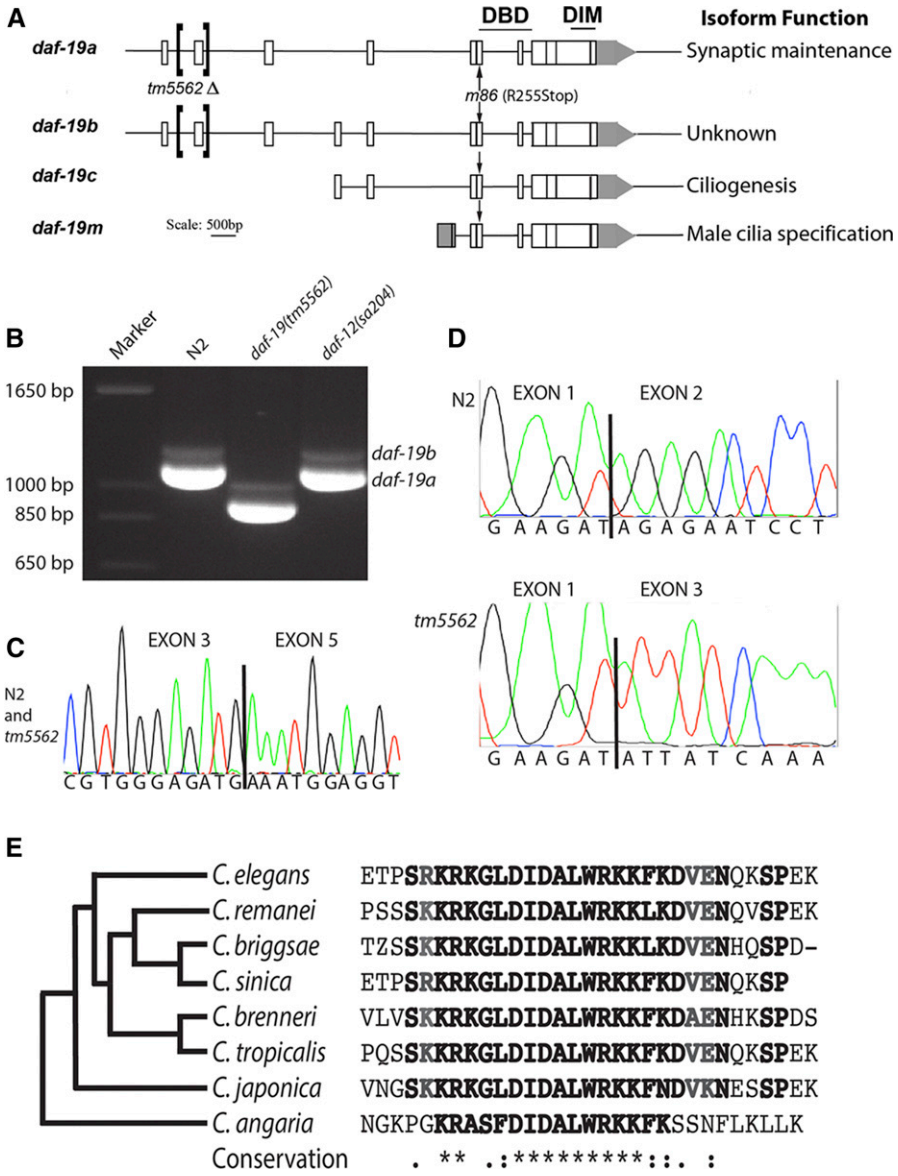

Figure 1 *daf-19* structure and characterization of *daf-19*(*tm5562*) RNA products. (A) Three promoters produce four related *daf-19* RNA products, as shown. Conserved DNA-binding (DBD) and dimerization (DIM) domains are indicated above encoding exons; locations of a new deletion allele *tm5562* and the null allele *m86* are noted with brackets and arrows, respectively. (B) Reverse transcription (RT)-PCR using primers to exons 1 and 10 reveal a highly abundant 1123-bp *daf-19a* transcript from worms wild-type for *daf-19*, a 934-bp transcript from *tm5562* worms, and a much less abundant *daf-19b* product that is 75-bp larger. (C) Sequencing trace from the smaller RT-PCR product shows splicing of exon 3–5 as in *daf-19a*. (D) Sequencing traces of exon 1 splicing in *daf-19a* cDNA products from wild-type N2 (top) and *daf-19*(*tm5562*) worms (below). (E) Translated sequences from exon 2 of *daf-19* orthologs aligned using T-Coffee (Di Tommaso *et al.* 2011) and clustered (left) according to the phylogeny of Slos *et al.* (2017). Sequence identifiers: *C. elegans*, gil71988112; *C. remanei*, gblEFP05251.1; *C. briggsae*, emblCAP22350.4; *C. sinica*, scaffold 899; *C. brenneri*, gblEGT33833.1; *C. tropicalis*, scaffold 563.1; *C. japonica*, contig 15741.5; and *C. angaria*, contig 57337_2.

and dead eggs. Threefold-stage embryos were further grown on OP50-seeded NGM agarose plates for 5 hr to obtain selectively enriched L1-stage worms. To obtain adult-stage worms, a synchronized hypochlorite-treated population was grown to the L4 stage on NGM agarose plates. Worms were gently rinsed from plates and gravity-settled for 5 min, washed with M9, and settled for 3 min, followed by a repetition with 1 min of settling. Early-stage larvae and embryos were left in each supernatant. This procedure was repeated after worms fed on agarose media for another 24 hr. Two-day-old well-fed adults were harvested 50 hr past the L4 stage.

RNA extraction, cDNA preparation and labeling, and microarray data generation

Harvested worms were passed through three freeze and thaw cycles using liquid nitrogen. For reverse transcriptase (RT)-PCR and microarray analysis, total RNA from the L1 stage was isolated using a standard phenol–chloroform extraction procedure following homogenization; total RNA from adults was prepared using TRIzol followed by a QIAGEN (Valencia, CA) RNAeasy kit following the manufacturer's directions. The quantity and quality of the extracted RNA was determined using an Agilent Bioanalyzer 2100 (Agilent, Santa Clara, CA). A standard eukaryotic target preparation protocol using 5 μg of total RNA was conducted for each array, as described in the Affymetrix GeneChip Eukaryotic Sample labeling protocol (Affymetrix). Four independent RNA preparations from L1 larvae and three from adults of each strain were used for one GPL200 Affymetrix *C. elegans* genome array hybridization each; array data were analyzed as described in the GeneChip Expression Analysis technical manual (Affymetrix). *In vitro* transcription, fragmentation, hybridization, staining, and scanning were performed by the Bioinformatics and Expression Analysis core facility, Karolinska Institute, Stockholm-Huddinge, Sweden (www.bea.ki.se). Primers for RT-PCR analysis of *daf-19* were

5′-GCCATCGACGAGCAGTGTG-3′ and 5′-CATGCAAGGAGA GACGCTG-3′. Additional primers for sequencing were 5′-CTTAC GAGGTGTTCCAGACGA-3′, 5′-TCGTCTGGAACACCTCGTAAG-3′ and 5′-AGACGGATCGGATGAGCTTTC-3'. RT-PCR used the SuperScript III One-Step RT-PCR system (Invitrogen, Carlsbad, CA).

Transcriptome analysis

Subsequent to scanning, microarrays were subjected to a range of low-stringency analyses, including image analyses, signal summarization, and normalization. Expression reports were examined to confirm that all internal control values were within the acceptable range, as defined by the Affymetrix Data Analysis Fundamentals (Affymetrix). Data passing all quality control measures were utilized for further statistical analyses.

CEL files obtained from microarray hybridizations were imported into robust multichip average (RMA) Express (version 0.3; http://rmaexpress.bmbolstad.com), and expression signal values were calculated using an RMA expression summary and quantile normalization technique. BRB Array Tools (version 3.3; http://linus.nci.nih.gov/BRB-ArrayTools.html) were used to identify genes with statistically signiφicant variation in expression. The probability threshold was set at a maximum of 0.05 (P-value ≤ 0.05) for genes to be considered statistically differentially expressed in wild-type and mutant populations. Genes with a signal variation of 1.5-fold or greater were selected for subsequent experiments. To reduce false discoveries, a class comparison test was conducted using a multivariate permutation test with a confıdence level of 97% (L1 analysis) and 90% (adults). This analysis revealed that 403 probes identified 370 unique differentially regulated genes ($n = 235$ downregulated and $n = 135$ upregulated) in *daf-19* mutant L1 larvae. Such a permutation is very similar to that utilized by the Significance Analysis of Microarrays (SAM) analyses (Tusher *et al.* 2001). Additional lists of genes were generated using SAM (version 2.2) with a false discovery rate (FDR) of $\leq 5\%$ (Q-value $\leq 5\%$) for L1 analysis and 10% for adult analysis. Thirty repeated runs of SAM were performed using variable random seed numbers for each run. During each run of SAM, 100 permutations were performed. Probes appearing with a bootstrap frequency of 24 (80% of total runs) were further considered for signal variation filtering, used to selectively identify genes with a 1.5-fold or greater variation between the two genetic conditions (L1 larvae: $n = 154$ downregulated and $n = 58$ upregulated). The list of genes differentially regulated in adults was generated similarly: RMA normalization followed by class comparison with a multivariate permutation, a FDR of 0.1 and 70% confidence level ($n = 120$ downregulated genes, $n = 75$ upregulated). SAM analysis yielded a list of 119 unique genes ($n = 74$ downregulated; $n = 45$ upregulated) that is completely contained within the larger list of differentially regulated genes. Comparisons between transcriptomes (threefold-stage embryos, Phirke *et al.* (2011); L1 larvae, this work; and adults, this work) were undertaken using the gene lists generated by class comparison (Table S2, Table S3, and Table S4).

Transcriptional GFP-fusion gene expression constructs

Gene expression was assessed exclusively using transcriptional GFP reporter constructs generated by inserting 1–3 kb of DNA upstream of genes of interest into the poly-cloning site of the GFP reporter plasmid pPD95.75 (Table S5). Germline transformations by microinjection (Mello *et al.* 1991) used one of two methods. In one set, GFP constructs (40 ng/μl) and the transformation marker *elt-2p*::*mCherry* [10 ng/μl; gift from Gert Jansen; Burghoorn *et al.* (2010)] were microinjected with carrier DNA at 50 ng/μl. Worms expressing mCherry in the intestine were analyzed for GFP expression. Alternatively, GFP constructs (70 ng/μl) were co-injected with 30 ng/μl *unc-122p*::*DsRed* with no carrier DNA. Worms with DsRed expression in coelomocytes were analyzed for GFP expression. Transgene GFP expression patterns were characterized in ≥ 30 L1 adult-stage worms per strain using a Leica TCS SP5 II confocal microscope; adult expression patterns are shown. For *gakh-1* and *del-4* age-dependent expression analysis, $N = 130$ and 40 per strain, respectively. Worms were immobilized using 10 mM NaN_3 on 2.0% agarose pads. Two *daf-19* translational constructs fused isoform-specific endogenous promoters to partial cDNAs expressing either *daf-19a* (pGG67_3) or *daf-19c* (pGG14) [described in Senti and Swoboda (2008)]; these two constructs were used for isoform-specific rescue experiments.

Dye-filling and behavioral assays

Fluorescent dye-filling assays: Starich *et al.* (1995) using DiI (Molecular Probes, Eugene, Or) were used to confirm cilia defects in *daf-19* mutant animals and to assist with neuronal identification in wild-type worms.

Dauer formation assays: Twenty gravid hermaphrodites were placed on OP50 for 6 hr, and dauer larvae were enumerated after 5 days (15°), 4 days (20°), or 3 days (25°) of growth. Tukey's pairwise comparisons of arcsine-transformed data were used to detect differences in average dauer production between strains for three replicate experiments. All behavioral and life history assays were done blind to strain identity.

Early life history: Thirty gravid hermaphrodites were placed on OP50 for 2 hr to produce tightly synchronized populations. The life stage of each offspring was assessed every 8 hr. Tukey's pairwise comparisons were used to detect significant differences in percent of worms at particular life stages in three replicate experiments.

Roaming assays: L4 worms were grown on fresh OP50 lawns for 12 hr, after which 30 adult worms were individually picked to the center of a bacterial lawn and allowed to forage for 1 hr at 19° and constant humidity. The proportion of OP50-covered 5-mm squares crossed by tracks was enumerated (cf. Senti and Swoboda 2008). Replicate assays were repeated on seven different dates. Data were arcsine-transformed for statistical analysis. Two-way ANOVA analysis

revealed assay date to be a significant variable; the behavior of each strain was compared using Tukey's pairwise comparisons for each assay date.

Aldicarb assays: Twenty hermaphrodites, 30 hr post-L4 stage, were placed on OP50-seeded NGM agar containing 500 μM aldicarb. Complete paralysis of the head was scored as in Mahoney *et al.* (2006). Data from each of six replicate assays were compared using a survivorship curve comparison test (Pyke and Thompson 1986).

Data availability

All microarray data sets were submitted to the Gene Expression Omnibus database (Edgar and Barrett 2006) under accession number GSE96068. *C. elegans* strains (Table S1) are available upon request. Gene lists generated from this study as well as from Phirke *et al.* (2011) are included in Table S2, Table S3, and Table S4. Table S5 lists all the primers used and Table S6 lists transgene constructs with apparent DAF-19-independent expression.

Results

Identification of DAF-19 target genes in L1 larvae and adult worms

To identify novel DAF-19 target genes, we employed whole-genome microarrays of *daf-19*(*m86*) null mutants and isogenic wild-type worms from synchronized L1 larvae and 2-day old adults. To add to the comparably prepared gene lists from embryos (Chen *et al.* 2006; Phirke *et al.* 2011 in Table S2), a comparison of mutant and wild-type populations (cf. *Materials and Methods*) uncovered large sets of differentially regulated genes in L1 larvae (Table S3) and adult worms (Table S4).

We determined whether DAF-19-regulated transcriptomes were enriched for particular types of genes and whether that enrichment changed during development. We found that the breadth of gene categories represented by DAF-19-regulated transcriptomes narrowed as development proceeded from embryos to L1-stage larvae to adults (Table 1). Based on the timing of ciliogenesis, we expected that DAF-19-regulated transcriptomes from embryos and L1 larvae would be enriched for genes involved in ciliogenesis, while this would not be the case for the adult-stage gene list. Such a finding would be consistent with the results from Jensen *et al.* (2016), who used a gene expression profiling approach to track ciliary gene expression during development. ;Our DAF-19-regulated transcriptome from L1-stage larvae was grouped into nine gene ontology clusters with enrichment scores > 1.5 (Huang *et al.* 2009), each containing ≥ 10 genes, including clusters representing cilia, dauer formation, signaling, and aging. By comparison, the DAF-19-regulated transcriptome from adults was enriched for smaller sets of genes involved in signaling, aging, and proteolysis. Both of these transcriptomes displayed an even stronger reduction in clusters when compared to the threefold-stage embryo DAF-19-regulated transcriptome (Phirke *et al.* 2011) (Table 1 and Table S2).

Comparisons with the Cilia database CilDB (Arnaiz *et al.* 2014) also indicated an enrichment of known ciliary genes in the gene list from L1 larvae, but not in the gene list from adults. Overall, CilDB identifies 15% of *C. elegans* genes as ciliary based on two or more published studies. Using the same criteria, we identified $> 21\%$ of the gene list from L1 larvae as ciliary, while only 11% of the adult gene list were known ciliary genes. Core ciliary genes (*e.g.*, *bbs* and *nphp* genes) important for the process of ciliogenesis (Choksi *et al.* 2014) were represented with statistical significance only on the gene lists from embyros and L1 larvae, indicating that the maintenance of cilia at the adult stage is very likely much less dependent on DAF-19 regulation. Lastly, there was significant enrichment (4–10-fold) in all three lists (threefold-stage embryo, L1 larvae, and adults) for genes expressed in neurons, with expression patterns becoming more restrictive as development proceeds (Figure S1). In light of the suggested function of DAF-19A/B in regulating the maintenance of protein levels at neuronal synapses, we note the presence in the adult gene list of 12 genes involved in proteolysis (Table 1), three of which we characterized in more detail: *spg-20*, *anp-1*, and *skr-12*.

For further analyses we chose a number of genes based on one of the following criteria: (1) a suggested neuronal expression pattern, (2) a WormBase annotation suggesting a connection to *daf-19* mutant phenotypes such as protein stability or innate immunity, or (3) no known function or expression pattern (see Table S5). In total, we assessed expression patterns of 44 candidate *daf-19* target genes using transcriptional GFP fusions, 32 of which have identified human orthologs (Shaye and Greenwald 2011). Out of the 44 genes, 33 showed strong GFP expression that was characterized further, whereby expression patterns were always compared between isogenic strains differing only by the *daf-19* allele. Gene choices were not filtered for their presence in an operon; four such genes were analyzed: three that are the first gene of an operon and one, *ddn-1*, that was the second [based on Allen *et al.* (2011)]. Characteristics of *daf-19* target genes and their expression patterns are summarized in Table 2 and Table S6.

The presence of DAF-19 activates gene expression

We compared the expression of putative target gene transcriptional fusions in *daf-19* null and wild-type genetic backgrounds to determine where and in which way target gene expression was DAF-19-dependent. Our transcriptome analysis revealed new genes activated in the nervous system in the presence of DAF-19. Seven gene promoter fusions showed clear evidence of activation by the presence of wild-type DAF-19 in neurons, mostly limited to subsets of CSNs (Table 2). The inner labial (IL2) neurons were a common site of *daf-19* target gene activation; expression of *asic-2*, *spg-20*, and *ddn-1* (downstream of *daf-19*) (Figure 2), as well as *ddn-2* [F35C5.11 in Phirke *et al.* (2011)] and *mapk-15*

Table 1 Annotation clusters of differentially regulated genes

Threefold embryo	Score	L1	Score	Adult	Score
Cilium assembly/dauer	10.67	Cuticle/collagen	12.04	Signal peptide	3.53
Cilium biogenesis/protein transport	4.85	Cilium assembly/behavior	5.21	Aging	2.99
Mitosis/cell cycle	4.04	Cilium assembly/dauer	4.17	Proteolysis	1.69
Vulval location/dauer entry	3.85	Lipid modification	3.31	Lipase	1.52
Glutathione transferase	3.66	Disulfide bond/cuticle	2.08	172 IDs, 17 clusters	
Protein processing/ubiquitin	3.24	Signal peptide	1.85		
Cilium morphogenesis/behavior	3.21	Aging	1.82		
Glucuronidation	3.08	Proteolysis	1.52		
Cytoskeleton	2.86	Neuropeptide	1.48		
Endoplasmic reticulum	2.54	364 IDs, 37 clusters			
Spindle/polar body extrusion	2.48				
Nucleosome	2.45				
ER lumen	2.22				
Histone	2.03				
Oxidoreductase	2.03				
Kinetochore/centromere	1.97				
Tetratricopeptide-like helical	1.91				
Cyclin	1.90				
Glucose/ribitol dehydrogenase	1.77				
EF-hand domain	1.68				
ATP-binding	1.54				
909 IDs, 21 clusters > 1.5					

Gene annotation clusters of differentially regulated genes. Genes identified as putative targets of *daf-19* in threefold stage embryos (Phirke *et al.* 2011), L1 larvae, and 2-day-old adults were clustered using the DAVID Bioinformatics Resource 6.7 with a medium classification stringency (Huang *et al.* 2009). Clusters with scores of ≥ 1.5 are shown. IDs, identifiers; DAVID, database for annotation, visualization and integrated discovery; ER, endoplasmic reticulum.

(Piasecki *et al.* 2017), in IL2 neurons required *daf-19*. IL2 neuron identity was confirmed by colocalization with a *cho-1*::*mCherry* reporter (Pereira *et al.* 2015) or lack of colocalization with *eat-4*::*mCherry* (Serrano-Saiz *et al.* 2013) (Figure S2). *ddn-1*::*gfp* is also differentially expressed in other CSNs; we observed robust activation in the presence of DAF-19 in ASG, and less pronounced activation in URX (not a CSN), ASI, and AFD, the latter identified by *eat-4* colocalization.

Even though DAF-19C is expressed in many or all CSNs and DAF-19A/B in nearly all nonciliated neurons (Senti and Swoboda 2008), all *daf-19* target genes examined appear to have RFX-independent expression in some neurons in addition to DAF-19 dependence in a subset of neurons (Table 2). For example, robust expression of *spg-20*::*gfp* was observed in the majority of neurons, but DAF-19-dependent activation was discernable only in IL2 neurons (Figure 2). Expression of *eppl-1*::*gfp* appeared DAF-19-dependent only in the CSNs ASE and ASG (Figure 2), but not in PQR or nonneuronal tissues, while DAF-19-dependent activation of *xbx-9*::*gfp*, found in our gene lists and previously described by Burghoorn *et al.* (2012), was restricted to three of four CSNs in which expression was observed. Finally, *del-4*::*gfp* expression was age-dependent in ASE, ASG, and several other unidentified neurons (Figure 2 and Table 2). ASE and ASG were identified by location, morphology, and by elimination: they do not dye-fill and are not cholinergic (Figure S2). In wild-type animals, *del-4* expression decreased from eight amphid CSNs in L1–L2 larvae to half as many in adults. In *daf-19*(*m86*) null mutant worms, no more than three neuron pairs expressed *del-4* in young larvae, and only one or two AIA neurons did so in adults. We conclude that DAF-19 activates *del-4* expression in ASE and in AIY interneurons. In other studies, *del-4* transcripts were found in ASE following serial analysis of gene expression (SAGE) analysis, and the gene contains an ASE motif (Etchberger *et al.* 2007) as well as an X-box motif (Efimenko *et al.* 2005).

DAF-19 presence downregulates some genes in the nervous system

Because two RFX orthologs in humans and yeast have been found to repress gene expression, we assessed expression patterns of several genes that appeared to be upregulated in the absence of DAF-19 in our gene lists. For the first time, we report that wild-type DAF-19 can downregulate target gene expression in both ciliated and nonciliated neurons. Three genes, all of which showed differential transcription in at least two life stages, were expressed in fewer neurons in wild-type worms than in *daf-19*(*m86*) null mutants. One additional gene, *mapk-15*, not identified by microarray analysis, was also downregulated by DAF-19 (Table 2).

daf-19-dependent downregulation of *skr-12* was seen in more than four sets of CSNs. Based on *eat-4* colocalization, we identified *skr-12* expression in the CSNs IL1, ASG, and AFD, and occasionally in the OLQ neurons in *daf-19*(*m86*) null mutants (Figure 3 and Figure S2). The characteristic microvilli at the tip of the AFD dendrites (Doroquez *et al.* 2014) were easily visible (Figure 3). Expression in two other CSNs, most likely ASE and ADF, was also downregulated by the presence of DAF-19. Two additional neurons in which *skr-12* was downregulated could not be identified due to faint expression levels. Expression of *skr-12* in the ASI and

Table 2 ***daf-19*-dependent target genes**

C. elegans Gene IDs	Gene function	Mutant/WT fold-change 3X[a]	L1	Adult	Cilia database	Expression pattern in wild-type worms	Expression pattern in *daf-19*(*null*) worms
asic-2 T28F4.2 191981_at	Predicted sodium channel	0.76	**0.54**	**0.65**	Yes	**IL2 neurons**, two fainter OLs	Two faint OLs
spg-20 F57B10.9 185820_at	Orthologous to SPARTIN	1.09	1.24	**1.58**	Yes	**IL2 neurons**, most neurons posterior of nerve ring, body wall muscle	Most neurons posterior of nerve ring, body wall muscle
ddn-1 B0507.10 180569_at	Unknown	1.17	**0.29**	1.02	No	**IL2, ASG, URX (rarer), AFD (faint), ASI (faint)**, ASE, I5, M5, intestine, muscle	ASE, I5, M5, intestine, some muscle
eppl-1 T01B11.2 190153_s_at	Transaminase activity	0.89	**0.62**	1.16	Yes	**ASG, ASE**, one tail neuron (PQR), pharynx, intestine, hypodermis	Tail neuron (PQR), pharynx, intestine, hypodermis
del-4 T28B8.5 190395_at	Predicted sodium channel	1.14	**0.40**	1.33	Yes	**ASE, AIY,** ASG (fainter), AIA, PHA, PQR (up to three neurons in tail)	AIA, ASG, up to three per head neurons in L1; 0–Two head neurons in adults, up to four tail neurons at all ages
mapk-15 C05D10.2 none	Mitogen-activated protein kinase	N/A	N/A	N/A	No	**IL2,** OLQ, CEPD/V, ASK, AFD, ADF, ADL, ASG, ASI, ASH, ASE, ADE, **PHA, PHB,** PQR	OLQ, CEPD/V, ASK, AFD, ADF, ADL, ASG, ASI, ASH, ASE, ADE, PQR
ddn-2 F35C5.11 184057_at	TGF-B activated receptor	**0.17**	**0.20**	**0.65**	Yes	**ILs**, two/three amphids, intestine	Two/three amphids, Intestine
xbx-9 C15C8.1 179348_at	unknown	**0.44**	**0.35**	0.82	Yes[a]	**3 CSNs,** ADF	ADF
skr-12 C52D10.6 189189_s_at	Homolog of SKp1, ubiquitin-ligase complex	**2.11**	0.96	0.55	No	ASI, ASK (rarer), intestine and pharynx	**IL1s, OLQs (rarer), AFD, ADF, ASG, ASE,** ASI, ASK, intestine, parts of pharynx
gakh-1 F46G11.3 192321_s_at	Cyclin G-associated kinase	**0.47**	**0.67**	**0.45**	Yes[a]	AIY (v. rarely), RIF, two–four tail neurons in adults. L3 have up to six GFP+ head neurons.	**URA, URB, IL2 (larvae only), BAG (<L4), AVA (rarer), AVB, SIAD/V, AIN (rarer), M4 (rarer), AIY,** RIF, 2–4 tail neurons
rgs-8.1 F52D2.2 189970_s_at	Regulator of G protein signaling	**0.66**	0.85	**0.34**	Yes	PVT, faint intestine	**RID, I2, 1 DV neuron, PVQ, PQRL/R,** faint intestine
mapk-15 C05D10.2 none	Mitogen-activated protein kinase	N/A	N/A	N/A	No	Much less robust in IL1	**IL1**

Summary of target gene expression. Characteristics and observed expression patterns of *daf-19* target genes are summarized. Gene functions were obtained from WormBase WS258. Fold-change is mutant versus wild-type expression (Phirke *et al.* 2011). Identification as a ciliary gene in Cilia database v. 3 (Arnaiz *et al.* 2014) is indicated. Expression patterns are summarized from at least 30 worms per strain equally divided by L1/L2, L3, L4, and adult life stages, except *gakh-1* and *del-4*, where N = 130 and 45, respectively. Genetic backgrounds were *daf-19-12*(*sa204*) with a *daf-19* null background [*daf-19*(*m86*)], or *daf-19*(+/+), where some age-dependent differences in expression were noted. Sites of differential expression (fold-change differences ≥ 1.5-fold) are highlighted in bold.

[a] Phirke *et al.* (2011) only.

ASK amphid CSNs (identified through colocalization with DiI), as well as in the intestine and pharyngeal muscle, appeared to be *daf-19*-independent.

daf-19-dependent downregulation of *gakh-1* was observed consistently in nonciliated neurons in an age-dependent manner. In wild-type adults, *gakh-1*::*gfp* was always expressed in the cholinergic RIF neurons and, rarely, in the AIY interneurons and the M4 pharyngeal motor neuron (Figure 3 and Figure S2). However, in *daf-19*(*m86*) mutants, the transgene was expressed in at least four additional sets of interneurons: AVB, AIY, AIN, and AVA (both less frequently), and either the SIAD and SIAV interneurons or possibly the SMBD motor neurons (Figure 3 and Figure S2). These latter neurons could not be unambiguously distinguished using *cho-1*::*mCherry* colocalization or by their morphology, but they never expressed *gakh-1* in wild-type worms (N = 132). In L3 and younger larval *daf-19* mutants, additional neuronal expression was seen in the glutamatergic BAG CSNs and, at low levels, in *cho-1*-expressing neurons anterior to the nerve ring (Figure S2). Sieburth *et al.* (2005) also reported *gakh-1*

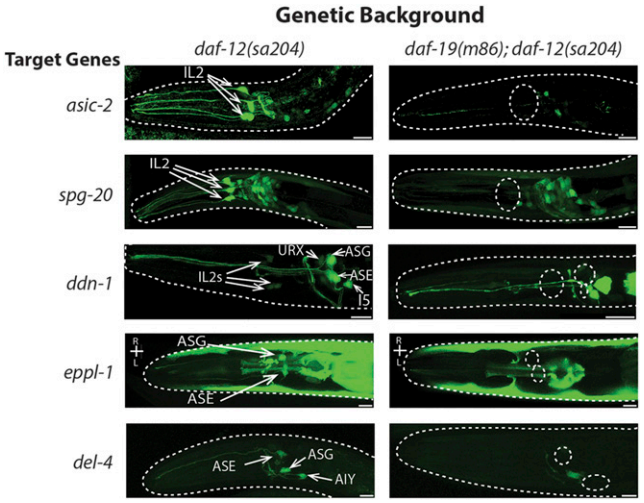

Figure 2 Presence of DAF-19 activates expression of novel target genes in certain ciliated sensory neurons. Expression patterns of transcriptional fusions of *daf-19* target gene promoters with the GFP gene in isogenic *daf-12*(*sa204*) and *daf-19*(*m86*); *daf-12*(*sa204*) adult hermaphrodites (*N* = 30 worms/strain analyzed). Views are lateral with dorsal at the top and anterior to the left, except strains expressing *eppl-1*::*gfp*. Neurons in which *daf-19*-dependent expression was found are identified. Cell bodies in which gene expression is absent in *daf-19*(*m86*) mutants are indicated by dotted circles. Bar, 10 μm.

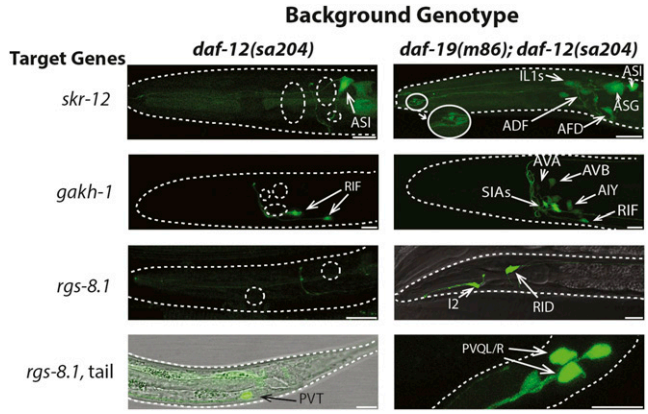

Figure 3 DAF-19 presence downregulates expression of novel target genes in certain nonsensory neurons and ciliated sensory neurons. Expression patterns of transcriptional fusions of *daf-19* target gene promoters with GFP in isogenic *daf-12*(*sa204*) and *daf-19*(*m86*); *daf-12*(*sa204*) adult hermaphrodites (*N* = 30 worms/strain analyzed, except for *gakh-1*, *N* = 130). Views are lateral with dorsal at the top and anterior to the left. Neurons in which *daf-19*-dependent expression was found are identified. Cell bodies in which gene expression is absent in worms wild-type for *daf-19* are indicated by dotted circles. Microvilli at the dendritic tips of AFD sensory neurons (in the right *skr-12* image) are magnified an additional 2×. Bar, 10 μm.

expression in the intestine, pharynx, and head and tail neurons in wild-type worms.

Only in *daf-19* mutant worms, *rgs-8.1*::*gfp* was consistently expressed in the I2 pharyngeal and nonciliated RID head neurons, as well as less frequently in four neurons of the tail (Figure 3 and Figure S2), including the PVQ interneuron pair, one of the DVA, B, or C neurons, and a single neuron directly posterior of PVQ. Expression in the PVT tail neuron was irregular in both wild-type and *daf-19* mutant backgrounds. *rgs-8.1* was also found to be differentially regulated in embryonic *daf-19*(*m86*) null mutant transcriptomes (Chen *et al.* 2006; Phirke *et al.* 2011).

In summary, expression of four target genes is downregulated only in the presence of DAF-19. This downregulation is specific to the nervous system.

Characterization of genes whose expression is (largely) independent of DAF-19

Fifteen gene promoter fusions yielded GFP expression in neurons that was (largely) independent of DAF-19 (Figure S3 and Table S6). This holds true also for genes expressed in both neurons and the intestine, or for genes (predominantly) expressed in the intestine, where they might be involved in innate immunity (Xie *et al.* 2013) (Figure S3 and Table S6). Three genes, *anp-1*, *hex-1*, and C06G3.6, showed a clear reduction in the frequency of neuronal expression in a *daf-19*(*m86*) null mutant background (Table S6). Seven genes were expressed in the intestine and not the nervous system, and another 14 were expressed in both tissues. In no case could we detect *daf-19*-dependent expression in the intestine (Table S6), even when neuronal expression was dependent on the presence of functional DAF-19 (*N* = 5 genes; Table 2). Similarly, though *daf-19* has been reported to be expressed to some extent in body wall muscle and hypodermis (Senti and Swoboda 2008), expression of target genes in either tissue was indistinguishable between wild-type and *daf-19*(*m86*) null mutants (Table S6). Apparent DAF-19 independence of putative target gene expression could be due to incomplete control regions in our transcriptional fusion constructs, DAF-19 dependence only at embryonic stages of development that were not fully assessed, or false positives in the microarray data. Thus, our experiments revealed *daf-19*-dependent target gene expression in the nervous system only.

Characterization of tm5562, an isoform-specific allele of daf-19

To determine which of the abundant DAF-19 isoforms (A or C) is responsible for controlling target gene expression, we characterized a new *daf-19* allele, *tm5562* (Figure 1). *tm5562* alters both *daf-19a* and *b* transcripts via deletion of exon 2, 582 bp of intron 1, and 93 bp of intron 2. RT-PCR revealed that *tm5562* mutant worms produced RNAs shorter than wild-type by the predicted length of exon 2 (Figure 1B). Both *daf-19a*, in which exon 3 is spliced to exon 5, and the *daf-19b* isoform including exon 4 were affected (Figure 1, B–D). Only in RNA isolated from *tm5562* mutants was exon 1 perfectly spliced to exon 3 in both isoforms (Figure 1D). Sequencing of RT-PCR amplicons as well as of genomic DNA revealed no other mutations through the DBD (data not shown). The *tm5562* transcript is expected to produce in-frame proteins lacking the evolutionarily conserved exon 2 (Figure 1E).

We determined that *daf-19*(*tm5562*) confers phenotypes expected of a *daf-19a* but not a *daf-19c* mutant, such as

roaming and pharmacological defects previously reported (Senti and Swoboda 2008). Wild-type worms will both dwell in small areas of a bacterial lawn and will roam to (Ben Arous *et al.* 2009), or explore (Flavell *et al.* 2013), new areas. We quantified the roaming behavior of individual worms and detected a significant difference between strains (Figure 4, A and B). *daf-19*(*tm5562*) worms displayed less roaming behavior than did wild-type N2 worms on all seven assay dates ($P < 0.003$). In all assays, *daf-19*(*tm5562*) behavior was either indistinguishable from that of *daf-19*(*m86*) null mutants ($P > 0.5$) or displayed an intermediate phenotype, statistically distinguishable from both wild-type N2 ($P < 0.002$) and *daf-19*(*m86*) null mutants ($P < 0.02$). As was the case for *daf-19*(*m86*) (Senti and Swoboda 2008), the aberrant roaming behavior of *daf-19*(*tm5562*) worms was rescued by transgenic expression of a *daf-19a*-specific construct ($P < 0.03$) (Figure 4B).

We assessed synaptic function in *daf-19*(*tm5562*) mutants using resistance to aldicarb, a cholinesterase inhibitor. For comparison, *daf-19*(*m86*) 1-day-old adult worms were consistently resistant to aldicarb, though not to the level of age-matched *unc-29*(*e1072*) mutants lacking a subunit of the acetylcholine receptor (Figure 4C). Age-matched *daf-19*(*tm5562*) worms were resistant to aldicarb at levels statistically indistinguishable from those of *daf-19*(*m86*) worms in an average of six replicate assays ($P = 0.56$). This synaptic defect was rescued by transgenic expression of *daf-19a* ($P = 0.02$). Average aldicarb sensitivity of rescued worms was indistinguishable from that of wild-type N2 ($P = 0.56$) (Figure 4C).

We used the aldicarb assay to test whether *daf-19*(*tm5562*) is a hypermorphic or dominant negative allele. If so, we expect heterozygous *tm5562*/+ mutant animals to confer an aldicarb-resistant phenotype. Instead, we found that *daf-19*(*tm5562*/+) heterozygotes had a phenotype indistinguishable from that of wild-type N2 worms mated with the same fluorescently marked strain (Figure S4D) (cf. *Materials and Methods*). We conclude that *daf-19*(*tm5562*) is a hypomorphic or loss-of-function allele affecting both *daf-19a* and *b* isoforms.

As expected, the *tm5562* allele did not appear to affect *daf-19c* function. While the *daf-19*(*m86*) null allele confers a highly penetrant Daf-c phenotype (Swoboda *et al.* 2000), *daf-19*(*tm5562*) did not confer a Daf-c phenotype in the presence of food at any temperature tested (Figure S4A). Normal progression from the first to second larval stages thus indicates that *daf-19a/b* is not responsible for the developmental decision to enter the dauer larval stage. Animals lacking DAF-19C do not develop cilia and therefore CSNs that normally take up the fluorescent, lipophilic DiI can no longer do so. The fact that *daf-19*(*tm5562*) worms dye-filled normally in both amphids (Figure S4B) and phasmids (data not shown), and males mated readily with hermaphrodites, suggests normal cilia development. These phenotypes are consistent with expression of functional *daf-19c* transcripts in *daf-19*(*tm5562*) worms.

Because *daf-19* can affect development, we followed worm development in populations synchronized by a 2-hr time window (Figure S4C). We found that *daf-19*(*tm5562*)

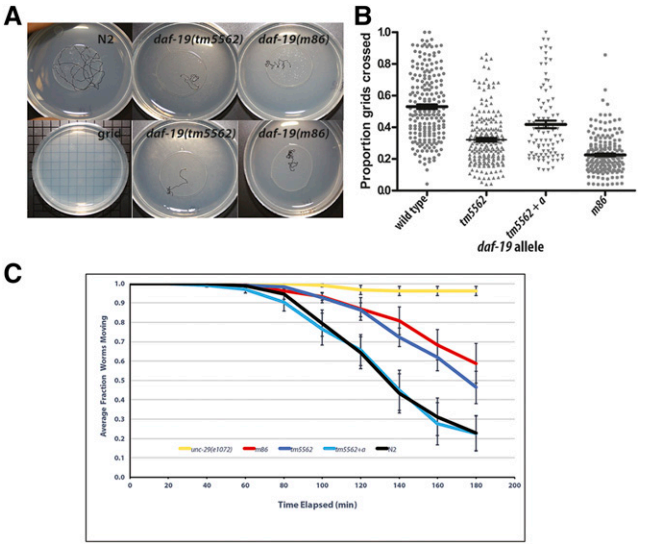

Figure 4 *daf-19*(*tm5562*) confers decreased roaming behavior and aldicarb resistance. (A) Each 1-day-old adult worm roamed freely from the center of an OP50 bacterial lawn for 1 hr at 19°: shown are representative worm tracks for worms of indicated genotypes. (B) Jitter plot of the proportion of grids crossed versus the total number of grids underneath the OP50 bacterial lawn; $N = 30$ worms per assay. *tm5562* + *a* indicates transgene expression of *daf-19a* from its endogenous promoter. The median and 1 SEM are indicated. Tukey's pairwise comparisons indicate that *tm5562* worms roam less than wild-type N2 worms on all assay dates ($P < 0.003$), while *tm5562* + *a* transgenic worms roam significantly more than *tm5562* worms ($P < 0.03$). (C) Response to 500 μM aldicarb was assessed as in Mahoney *et al.* (2006). Error bars are 1 SEM. Pairwise comparisons of average paralysis curves ($N = 6$ assays) were compared (Pyke and Thompson 1986). *tm5562* worms are not different from *m86* worms ($P = 0.56$), whereas *tm5562* + *a* transgenic worms differ from *m86* worms ($P = 0.02$) and do not differ from wild-type N2 worms ($P = 0.56$).

worms developed more slowly through the L3 stage, as indicated by the larger number of worms at this larval stage at 40 and 48 hr after egg laying ($P = 0.00023$ as compared to wild-type N2). We conclude that the time course of larval development of *daf-19*(*tm5562*) worms was slightly altered. Similar phenotypes, notably an L2 stage extension, have been found for Daf-c temperature-sensitive mutants of *daf-2*, when at the permissive temperature these worms do not enter the dauer stage (Ruaud *et al.* 2011; Olmedo *et al.* 2015). In summary, phenotypes conferred by *daf-19*(*tm5562*) are consistent with those of *daf-19*(*m86*) null mutant worms in which the *daf-19c* isoform is rescued by transgene expression (Senti and Swoboda 2008). These results indicate that the *tm5562* allele strongly reduces or eliminates solely the function of the longer *daf-19a* and *b* isoforms (cf. Figure 1A). Rescue of *tm5562* phenotypes by *daf-19a* expression suggests that DAF-19A plays an important and unique role in nervous system function.

daf-19 isoform-specific regulation of target gene expression

We used the *daf-19*(*tm5562*) genetic background to determine whether differential target gene expression required functional DAF-19A. For six target genes for which the

presence of DAF-19 activated expression, we compared the expression patterns between *daf-19*(*tm5562*) mutants and *daf-19*(*m86*) null mutant worms that carried isoform-specific rescuing transgenes [notated as *daf-19*(*0*)+*a* or +*c*]. With no exceptions, these six target genes remained activated in a *daf-19*(*tm5562*) background (Figure 5 and Table 3). Consistent with this finding, the activated expression of these six target genes was rescued in *daf-19*(*0*)+*c* animals, whereas in *daf-19*(*0*)+*a* animals it was not rescued. Surprisingly, transgenic overexpression of *daf-19a* repressed the near-pan-neuronal expression of *spg-20* as well as all expression of *asic-2* (Figure 5), a phenotype we term *ectopic repression* (Table 3).

In contrast, downregulation of target genes appeared to depend primarily, but not exclusively, on the action of DAF-19A. In *daf-19*(*tm5562*) mutant worms, *skr-12* and *gakh-1* were highly expressed; that is, they were not repressed in a *daf-19a* mutant background, but they were repressed in an isogenic wild-type background (Figure 5 and Table 3). Overexpression of *daf-19c* did not change this lack of repression of *gakh-1* and, usually, *skr-12*. In a few animals, *skr-12* was repressed such that expression was limited to the ASE neurons (Figure 5). Overexpression of *daf-19a* fully rescued repression of *gakh-1*, yielding gene expression patterns exactly like that seen in wild-type worms, while repression of *skr-12* expression by the presence of DAF-19A was more extensive than the wild-type pattern (Figure 3 and Figure 5). Thus, *skr-12* and *gakh-1* repression depended on functional DAF-19A.

To our surprise, *rgs-8.1* expression in I2 and RID neurons could be repressed in the presence of either isoform of DAF-19. Expression in I2, RID, and in tail neurons was repressed in *daf-19*(*tm5562*) worms as well as in both *daf-19*(*0*)+*a* and +*c* worms. These data suggest that a particular stoichiometry of DAF-19 proteins is important for the correct expression of *rgs-8.1*. Note that in all cases, transgene presence was ascertained by the presence of the corresponding co-injection marker (cf. *Materials and Methods* and Figure 5). Lastly, a parallel project revealed that a kinase gene, *mapk-15*, appeared to be both activated and repressed by the presence of DAF-19. In the presence of DAF-19, *mapk-15* is activated in IL2, PHA, and PHB, and many male tail CSNs, but is partially downregulated in IL1s and some of the neurons in the male tail (Piasecki *et al.* 2017). Expression in other CSNs, including many amphid head and the PQR tail CSNs, does not depend on DAF-19. We found *mapk-15* activation in *daf-19*(*tm5562*) and in *daf-19*(*0*)+*c* worms, but not in *daf-19*(*0*)+*a* worms. Instead, overexpression of *daf-19a* repressed nearly all *mapk-15* expression in the head, with variable repression in the hermaphrodite tail and no repression in the male tail, again suggesting that DAF-19 stoichiometry is important for correct gene expression in some neurons.

We conclude with the novel finding that expression of the DAF-19A isoform downregulates certain target genes in nonsensory neurons, while DAF-19C expression generally activates genes in CSNs and can, albeit rarely and restricted to small sets of neurons, also downregulate gene expression. These results are consistent with the described, mutually exclusive expression patterns of these two DAF-19 isoforms (Senti and Swoboda 2008).

Discussion

Using comparative transcriptomics during different life stages of the worm *C. elegans*, we have uncovered large sets of new target genes for DAF-19, the sole RFX TF in this organism. We can assign a number of these target genes to act in defined sets of neurons and, for some, at certain time points during development. DAF-19-dependent expression of these target genes extends beyond CSNs and the threefold stage of embryogenesis, by which time most cilia are formed (Sulston *et al.* 1983; Nechipurenko *et al.* 2016). Our work thereby greatly expands the suggested roles for DAF-19 and its target genes beyond a role in ciliogenesis (Choksi *et al.* 2014). Specifically, the presence of the larger DAF-19A isoform downregulates target genes in nonciliated neurons in larval through adult stages, while the smaller DAF-19C isoform primarily activates target genes in particular subsets of CSNs. Thus, *daf-19* provides important contributions to the regulation and maintenance of neuron function throughout development and adulthood.

To determine which DAF-19 isoform regulates target gene expression, we characterized a novel *daf-19* allele, *tm5562*, a deletion of exon 2. The homozygous mutant confers neuronal phenotypes expected of a *daf-19a* mutant, *e.g.*, dwelling/roaming defects and aldicarb resistance, but does not affect ciliogenesis or confer abnormal dauer development as expected of a *daf-19c* mutation. Since *daf-19*(*tm5562*) lacks exon 2 and acts as a loss-of-function allele, we suggest that amino acids encoded by this exon play an important role in DAF-19A function. Sequence alignment of available *daf-19* orthologs in different *Caenorhabditis* species reveals a highly conserved block of 22 amino acids (Figure 1E) in exon 2. Conservation of this sequence ranges from 80 to 90%. The conserved sequence is rich in positively charged amino acids but contains no currently recognized protein motif.

DAF-19-dependent downregulation of neuronal gene expression in *C. elegans* is a newly described phenomenon. We identified new target genes, *skr-12*, *gakh-1*, *rgs-8.1*, and the recently characterized *mapk-15* (Piasecki *et al.* 2017), whose expression was downregulated by DAF-19A in a subset of neurons. In another study, downregulation by *daf-19* was reported for the gene *peli-1*, but only when a canonical proximal X-box promoter motif was removed, and a less conserved, more distal X-box remained (Chu *et al.* 2012). None of the three downregulated genes identified in our transcriptomics approach harbor an identified, canonical X-box promoter motif, while the *mapk-15* gene has a putative X-box motif (Blacque *et al.* 2005) located further upstream than is typical (Burghoorn *et al.* 2012; Piasecki *et al.* 2017). To what extent downregulation of target genes by *daf-19* depends on X-box motifs, protein-binding partners, or possible indirect effects will be the subject of future studies.

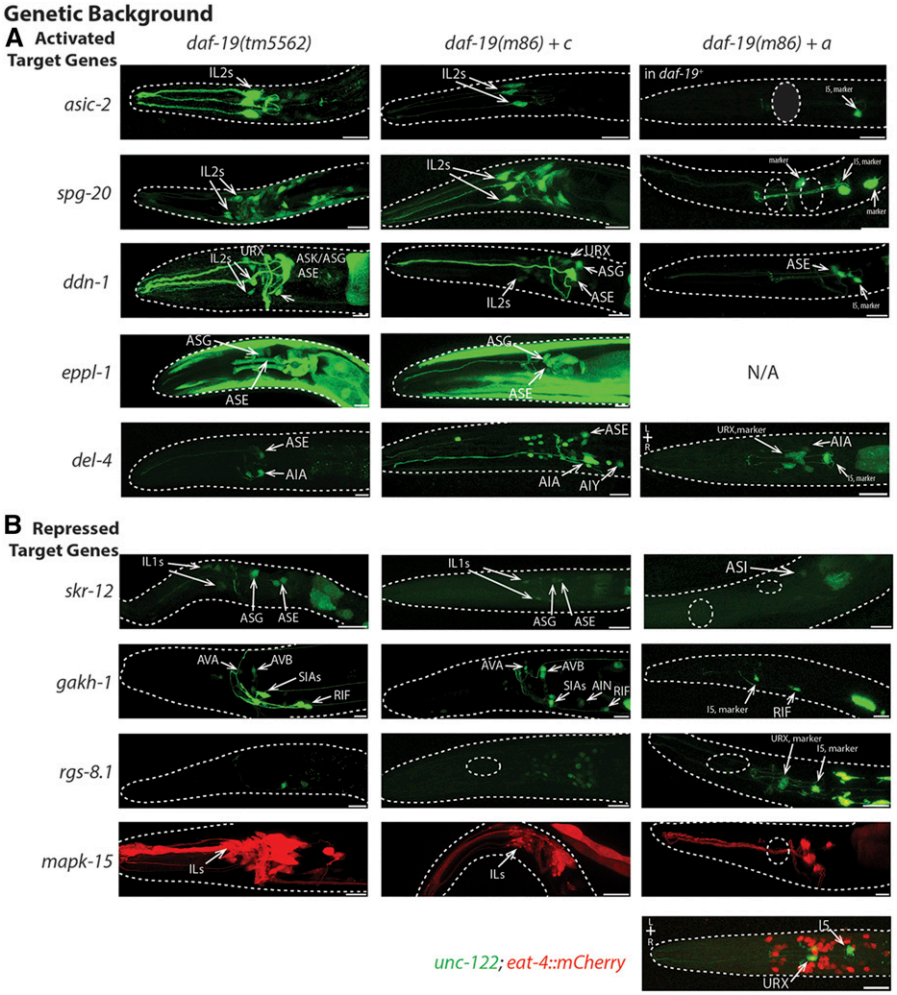

Figure 5 Isoform-specific control of *daf-19* target genes. (A) Target genes activated by the presence of DAF-19 are still activated in a *daf-19*(*tm5562*) background, where DAF-19C, but not DAF-19A, is functional. These genes are also activated when a transgene expressing DAF-19C, but not a DAF-19A transgene, is added to *daf-19*(*m86*) null mutant worms. Overexpression of DAF-19A represses expression of *asic-2*, *spg-20*, and *mapk-15* even in cells where expression is typically independent of *daf-19* (Figure 2). N/A = expression of target gene in muscle prevented identification of *daf-19a* co-injection marker. (B) Two target genes, *skr-12* and *gakh-1*, are repressed in a *daf-19* wild-type background, but are not repressed in a *daf-19*(*tm5562*) background when DAF-19A is nonfunctional. Expression of *rgs-8.1* and *mapk-15* is repressed in the presence of either isoform of DAF-19. Bar, 10 μm.

RFX TFs have been found to repress target gene expression in other organisms. Human RFX1 is capable of auto-repression regulated by DNA damage and replication blocking (Lubelsky *et al.* 2005). Yeast RFX, Crt1, is also a transcriptional repressor that can repress its own promoter and that of other genes (Huang *et al.* 1998). Similar regulatory pathways control repression by these proteins in both humans and yeast (Lubelsky *et al.* 2005). *C. elegans*, DAF-19 is most similar to human RFX1-4 (Choksi *et al.* 2014). The finding that DAF-19A expression downregulates or represses target genes is thus conserved, even if the biological pathways in which the respective RFX TFs act may differ. It will be of interest to know whether target gene repression is linked to neuronal identity, as described by Hobert (2010).

Activation of target gene expression was shown to require the shorter DAF-19C isoform, known to be necessary for ciliogenesis. Target gene activation is known to be mediated through a canonical *cis*-acting X-box promoter motif (Blacque *et al.* 2005; Efimenko *et al.* 2005; Chen *et al.* 2006), as well as a nearby C-box enhancer element (Burghoorn *et al.* 2012). However, we found that four of the eight genes that were activated by the presence of DAF-19C do not contain a canonical X-box. Though this finding is novel for target genes activated by DAF-19C, Wang *et al.* (2010) found that DAF-19M target genes lack a canonical X-box, and Xie *et al.* (2013) found that an isoform of *daf-19* activates the gene *tph-1* in the ADF neurons and antimicrobial genes in the intestine through an X-box-independent mechanism. These authors suggest that either DAF-19 regulates these target genes through a different DNA sequence motif, an unrecognized degenerate X-box, or by partnering through its dimerization domain with another TF. Given that *daf-19* lacks an apparent TF activation domain, the latter model appears likely. The fact that DAF-19 works with ATF-7 to regulate responses to pathogenic bacteria (Xie *et al.* 2013) lends further support to such a model. Alternatively, regulation of target genes that lack X-box motifs could be due to indirect effects of DAF-19C regulating other genes.

daf-19 alters gene expression in dauer-inhibiting and labial neurons

Mutations in TF genes often phenocopy neuronal ablation by causing misregulation of target genes, thereby affecting specific neuron function (Hobert 2016a). *daf-19* null mutants are Daf-c, thus, one might expect to see differential gene regulation in neurons that inhibit dauer entry. Bargmann and

Table 3 *daf-19* isoform-specific target gene regulation

		Expression in indicated worm genotype				
Gene name	Gene ID	Wild-type daf-19	*daf-19* (*tm5562*)	*daf-19(0)* + *daf-19c*	*daf-19(0)* + *daf-19a*	Interpretation
Target gene expression activated in the presence of daf-19						
asic-2	T28F4.2	Activated	Activated	Rescues activation	Ectopic repression	DAF-19C activates target gene; DAF-19A overexpression represses
spg-20	F57B10.9	Activated	Activated	Rescues activation	Ectopic repression	DAF-19C activates target gene; DAF-19A overexpression represses
ddn-1	B0507.10	Activated	Activated	Rescues activation	No rescue	DAF-19C activates target gene
eppl-1	T01B11.2	Activated	Activated	Rescues activation	N/A	DAF-19C activates target gene
del-4	T28B8.5	Activated	Activated	Rescues activation	Partial rescue	DAF-19C activates target gene
mapk-15	C05D10.2	Activated	Activated	Rescues activation	Ectopic repression in head	DAF-19C activates target gene; DAF-19A overexpression represses
Target gene expression repressed in the presence of daf-19						
skr-12	C52D10.6	Repressed	Activated	Activated	Ectopic repression	Repression requires DAF-19A; DAF-19A overexpression represses expression
gakh-1	F46G11.3	Repressed	Activated	Activated	Rescues repression	Repression requires DAF-19A
rgs-8.1	F52D2.2	Repressed	Repressed	Rescues repression	Rescues repression	Either isoform can repress
mapk-15	C05D10.2	Repressed	Activated	Activated	Repressed in head	Repression requires DAF-19A

Isoform-specific control of target gene expression. The average expression phenotype of *daf-19* target genes is shown in a *daf-19*(*tm5562*) mutant background (lacking functional DAF-19A) and in *daf-19* null (*m86*) worms expressing either *daf-19c* or *daf-19a* from their endogenous promoters. ID, identifier; N/A, *unc-122*p::gfp co-injection marker not detectable due to target gene expression in muscle.

Horvitz (1991) identified the ADF, ASI, and ASG neurons as repressing dauer development in noninducing conditions. Conversely the ASJ neurons are required for initiating dauer development (Schackwitz *et al.* 1996). Thus, we might expect to find-regulated gene expression in ADF, ASI, and ASG, but not in ASJ. We found that *ddn-1*, *eppl-1*, and *del-4* were strongly activated by the presence of DAF-19C in ASG, *ddn-1* was weakly activated by DAF-19C in ASI, and *skr-12* expression was downregulated in ADF (Table 4), while none of the *daf-19*-regulated genes studied here were differentially expressed in ASJ neurons. It will be of interest to determine whether any genes regulated by *daf-19* in this set of neurons are integral to the inhibition of dauer entry.

In addition, a large number of genes are regulated by *daf-19* in the labial neurons (Burghoorn *et al.* 2012; this study), known to generate dendritic arbors in dauer larvae and to direct dauer-specific behaviors (Schroeder *et al.* 2013). This suggests that further work could determine whether DAF-19 is one of the terminal selectors of labial neuron identity (cf. Hobert 2016b) as continued gene regulation in these neurons into adulthood suggests.

daf-19-dependent gene regulation in neurons involved in foraging and locomotion

Mutations in either major *daf-19* isoform are associated with aberrant roaming behavior, specifically overdwelling and increased turning based on observed worm tracks (Figure 4; Senti and Swoboda 2008). Thus, one might predict that *daf-19* target gene regulation would occur in neurons that inhibit dwelling and turning, or that stimulate roaming. That is, neurons, which upon ablation, lead to increased dwelling and reduced exploration would be expected to express DAF-19-dependent genes. These neurons include ASI and AIY, required to suppress reversals and turns associated with the local search state and dispersal (Gray *et al.* 2005; Cohen *et al.* 2009), and the ASE, ASI, and BAG neurons that function in adaptive food leaving behavior when food is depleted (Milward *et al.* 2011). In contrast, one would not expect to see *daf-19*-dependent gene expression in HSN or NSM in which *tph-1* is responsible for suppressing exploration (Flavell *et al.* 2013).

We found differential expression of *daf-19* target genes in neurons that both induce exploration and suppress dwelling behaviors. *ddn-1* and *del-4* were activated in the ASI and AIY neurons, respectively. Three genes were activated in the ASE neurons, while *gakh-1* was repressed by *daf-19a* expression in the BAG neurons in larvae (Table 4). As predicted, we did not observe target gene regulation in HSN or NSM.

daf-19 regulates genes involved in protein homeostasis

We hypothesized that misregulation of genes involved in protein homeostasis contributes to neuronal phenotypes of adult *daf-19*(*m86*) mutants, based on detectable synaptic protein loss in these animals (Senti and Swoboda 2008). Vayndorf *et al.* (2016) also demonstrated that neuron remodeling during aging is modified by compromised protein homeostasis. Gene ontology analysis of the differential transcriptome of adult worms (Table 1 and Table S4) yielded an overrepresentation of putative *daf-19* target genes with designations of ubiquitin and proteolysis. Of the 12 genes so identified, nine encode proteases or orthologs of the ubiquitin ligase system (http://www.wormbase.org). We analyzed

Table 4 Neurons in which *daf-19* controls target gene expression

Neuron	Target genes	Selected neuron functions
IL2s	*asic-2*, *spg-20*, *ddn-1*	Dauer behavior
URX	*ddn-1*	Suppresses innate immunity, life span regulation
ASK	*ddn-1*	Initiates local search behavior
AFD	*ddn-1*	Ablation causes hypo-reversal
ASG	*ddn-1*, *eppl-1*, *del-4*	Inhibits entry into dauer
ASI	*ddn-1*	Suppresses turning, promotes dispersal, modulates innate immune response
ASE	*del-4*, *eppl-1*, *ddn-1*	Food leaving behavior
AIY	*del-4*	Suppresses turns and reversals, regulates life span, starvation response
I5	*ddn-1*	Regulates pharyngeal muscle relaxation
M5	*ddn-1*	Unknown
PHA, PHB	*mapk-15*	Chemorepulsion, mate searching
IL1s	*skr-12*, *mapk-15*	Spontaneous and faster foraging
OLQs	*skr-12*	Spontaneous and faster foraging
BAG	*gakh-1*	Controls life span, food leaving behavior
AFD	*skr-12*	Ablation causes hypo-reversal
ADF	*skr-12*	Inhibits entry into dauer, modulates NMJ transmission
ASG	*skr-12*	Inhibits entry into dauer
I2	*rgs-8.1*	Unknown function
RID	*rgs-8.1*	Unknown function
AVA	*gakh-1*	Driver for backward locomotion
AVB	*gakh-1*	Driver for forward locomotion
SIAD/V	*gakh-1*	Nerve ring placement
AIN	*gakh-1*	Unknown function
M4	*gakh-1*	Posterior isthmus peristalsis

Neurons in which *daf-19* presence activates or represses target gene expression, and associated neuron functions [from Altun *et al.* (2002–2017)] relevant to *daf-19* mutant phenotypes. Neurons are listed top to bottom by their position in the worm, anterior to posterior. Ciliated sensory neurons are in bold. NMJ, neuromuscular junction.

expression patterns of three of these nine genes and found misregulation of all three in *daf-19* mutant backgrounds. *skr-12* is one of five SKP-1 ubiquitin ligase component orthologs (Edwards *et al.* 2009) in our adult differential transcriptome and it is downregulated by DAF-19A, while *spg-20* encodes an ortholog of human SPG20, a ubiquitin ligase component implicated in spastic paraplegia (Karlsson *et al.* 2014), which is activated by the presence of DAF-19C. We also observed partial DAF-19-dependent activation of *anp-1*, which encodes an aminopeptidase (Table S6). In addition, Chu *et al.* (2012) reported that DAF-19 regulates *peli-1*, which encodes a protein with similarity to an E3 ubiquitin ligase. Modulation of *peli-1* expression (Huang *et al.* 2002) is consistent with neuronal phenotypes associated with worms lacking only DAF-19A, while *spg-20* mutants display lower crawling and thrashing speeds and are more sensitive to paraquat (Truong *et al.* 2015). In the future, it will be of interest to determine whether mutations of these or other ubiquitin components alter synaptic protein homeostasis.

The work described here, along with that reported by Chen *et al.* (2006), Phirke *et al.* (2011), and Jensen *et al.* (2016), provides an exhaustive list of novel *daf-19* target genes at four points during worm development: from embryogenesis to the adult stage. We have characterized orthologs of human disease genes, including *spg-20* (SPARTIN), mutations of which cause a spastic paraplegia called Troyer syndrome in humans (Patel *et al.* 2002), and *gakh-1*, encoding a possible regulator of clathrin-mediated membrane trafficking. Mutations of an orthologous human cyclin G-associated kinase (GAK) gene are implicated in susceptibility to Parkinson's disease (Pankratz *et al.* 2009; Hamza *et al.* 2010). These two examples, but also others from our gene lists, will aid in studies of neuronal function and in understanding connections to human disease. Lastly, our discovery that DAF-19, the sole *C. elegans* RFX TF, modulates gene expression in nonciliated neurons opens up new avenues of research into the specification and function of nonsensory neurons.

Acknowledgments

E.A.D.S. thanks Bart De Stasio for statistical expertise and moral support, and the laboratory of Maureen Barr for a quiet place to write and wonderful colleagues, particularly Juan Wang for assistance with RT-PCR. Some worm strains were provided by the *Caenorhabditis* Genetics Center, funded by the National Institutes of Health (NIH) (P40 OD-010440). We acknowledge online resources, particularly WormBase and WormAtlas. Additional undergraduate students made contributions to this work: Kristen Bischel, Elisa Carloni, Christina Schaupp, and Lu Yu. E.A.D.S. was supported in this work by the NIH (R15 AG-16192-01) and by a Fulbright Research Fellowship with Sweden. A National Science Foundation (NSF)-Major Research Implementation grant (DBI 11-26711) to E.A.D.S., B.P.P., and colleagues provided a confocal microscope. Undergraduate summer stipends were provided by the NSF-Wisconsin Alliance for Minority Participation (402549) and Lawrence University. Work in the laboratory of P.S. was supported by the Swedish Research Council and by the Marcus Borgström, Torsten Söderberg, and Åhlén Foundations. P.S. also received support from

the Swedish Foundation for Strategic Research and the Karolinska Institute (KI) Strategic Neurosciences Program. D.S.-T. received support from the KI in the form of a Ph.D. student (KID) scholarship.

Literature Cited

Aftab, S., L. Semenec, J. S. Chu, and N. Chen, 2008 Identification and characterization of novel human tissue-specific RFX transcription factors. BMC Evol. Biol. 8: 226.

Allen, M. A., L. W. Hillier, R. H. Waterston, and T. Blumenthal, 2011 A global analysis of C. elegans trans-splicing. Genome Res. 21: 255.

Altun, Z. F., L. A. Herndon, C. A. Wolkow, C. Crocker, R. Lints *et al.*, 2002-2017 Wormatlas. Available at: http://www.wormatlas.org.

Arnaiz, O., J. Cohen, A. M. Tassin, and F. Koll, 2014 Remodeling Cildb, a popular database for cilia and links for ciliopathies. Cilia 3: 9.

Bargmann, C. I., and H. R. Horvitz, 1991 Control of larval development by chemosensory neurons in *Caenorhabditis elegans*. Science 251: 1243–1246.

Ben Arous, J., S. Laffont, and D. Chatenay, 2009 Molecular and sensory basis of a food related two-state behavior in *C. elegans*. PLoS One 4: e7584.

Blacque, O. E., E. A. Perens, K. A. Boroevich, P. N. Inglis, C. M. Li *et al.*, 2005 Functional genomics of the cilium, a sensory organelle. Curr. Biol. 15: 935–941.

Brenner, S., 1974 The genetics of *Caenorhabditis elegans*. Genetics 77: 71–94.

Burghoorn, J., M. P. J. Dekkers, S. Rademakers, T. de Jong, R. Willemsen *et al.*, 2010 Dauer pheromone and G-protein signaling modulate the coordination of intraflagellar transport kinesin motor proteins in *C. elegans*. J. Cell Sci. 123: 2076–2083.

Burghoorn, J., B. P. Piasecki, F. Crona, P. Phirke, K. E. Jeppsson *et al.*, 2012 The *in vivo* dissection of direct RFX-target gene promoters in *C. elegans* reveals a novel *cis*-regulatory element, the C-box. Dev. Biol. 368: 415–426.

Chen, N., A. Mah, O. E. Blacque, J. Chu, K. Phgora *et al.*, 2006 Identification of ciliary and ciliopathy genes in *Caenorhabditis elegans* through comparative genomics. Genome Biol. 7: R126.

Choksi, S. P., G. Lauter, P. Swoboda, and S. Roy, 2014 Switching on cilia: transcriptional networks regulating ciliogenesis. Development 141: 1427–1441.

Chu, J. S. C., D. L. Baillie, and N. Chen, 2010 Convergent evolution of RFX transcription factors and ciliary genes predated the origin of metazoans. BMC Evol. Biol. 10: 130.

Chu, J. S. C., M. Tarailo-Graovac, D. Zhang, J. Wang, B. Uyar *et al.*, 2012 Fine tuning of RFX/DAF-19-regulated target gene expression through binding to multiple sites in *Caenorhabditis elegans*. Nucleic Acids Res. 40: 53–64.

Cohen, M., V. Reale, B. Olofsson, A. Knights, P. Evans *et al.*, 2009 Coordinated regulation of foraging and metabolism in *C. elegans* by RFamide neuropeptide signaling. Cell Metab. 9: 375–385.

Craig, H. L., J. Wirtz, S. Bamps, C. T. Dolphin, and I. A. Hope, 2013 The significance of alternative transcripts for *Caenorhabditis elegans* transcription factor genes, based on expression pattern analysis. BMC Genomics 14: 249.

Di Tommaso, P., S. Moretti, I. Xenarios, M. Orobitg, A. Montanyola *et al.*, 2011 T-coffee: a web server for the multiple sequence alignment of protein and RNA sequences using structural information and homology extension. Nucleic Acids Res. 39: W13–W17.

Doroquez, D. B., C. Berciu, J. R. Anderson, P. Sengupta, and D. Nicastro, 2014 A high-resolution morphological and ultrastructural map of anterior sensory cilia and glia in *Caenorhabditis elegans*. Elife 3: e01948.

Edgar, R., and T. Barrett, 2006 NCBI GEO standards and services for microarray data. Nat. Biotechnol. 24: 1471–1472.

Edwards, T. L., V. E. Clowes, H. T. H. Tsang, J. W. Connell, C. M. Sanderson *et al.*, 2009 Endogenous spartin (SPG20) is recruited to endosomes and lipid droplets and interacts with the ubiquitin E3 ligases AIP4 and AIP5. Biochem. J. 423: 31–39.

Efimenko, E., K. Bubb, H. Y. Mak, T. Holzman, M. R. Leroux *et al.*, 2005 Analysis of xbx genes in *C. elegans*. Development 132: 1923–1934.

Elkon, R., B. Milon, L. Morrison, M. Shah, S. Vijayakumar *et al.*, 2015 RFX transcription factors are essential for hearing in mice. Nat. Commun. 6: 8549.

Emery, P., B. Durand, B. Mach, and W. Reith, 1996 RFX proteins, a novel family of DNA binding proteins conserved in the eukaryotic kingdom. Nucleic Acids Res. 24: 803–807.

Etchberger, J. F., A. Lorch, M. C. Sleumer, R. Zapf, S. J. Jones *et al.*, 2007 The molecular signature and cis-regulatory architecture of a *C. elegans* gustatory neuron. Genes Dev. 21: 1653–1674.

Flavell, S. W., N. Pokala, E. Z. Macosko, D. R. Albrecht, J. Larsch *et al.*, 2013 Serotonin and the neuropeptide PDF initiate and extend opposing behavioral states in *C. elegans*. Cell 154: 1023–1035.

Gajiwala, K. S., H. Chen, F. Cornille, B. P. Roques, W. Reith *et al.*, 2000 Structure of the winged-helix protein hRFX1 reveals a new mode of DNA binding. Nature 403: 916–921.

Garg, A., B. Futcher, and J. Leatherwood, 2015 A new transcription factor for mitosis: in *Schizosaccharomyces pombe*, the RFX transcription factor Sak1 works with forkhead factors to regulate mitotic expression. Nucleic Acids Res. 43: 6874–6888.

Gray, J. M., J. J. Hill, and C. I. Bargmann, 2005 A circuit for navigation in *Caenorhabditis elegans*. Proc. Natl. Acad. Sci. USA 102: 3184–3191.

Hamza, T. H., C. P. Zabetian, A. Tenesa, A. Laederach, J. Montimurro *et al.*, 2010 Common genetic variation in the HLA region is associated with late-onset sporadic Parkinson's disease. Nat. Genet. 42: 781–785.

Henriksson, J., B. P. Piasecki, K. Lend, T. R. Burglin, and P. Swoboda, 2013 Finding ciliary genes: a computational approach. Cilia. Pt B 525: 327–350.

Hobert, O., 2010 Neurogenesis in the nematode *Caenorhabditis elegans* (October 4, 2010), *WormBook*, ed. The *C. elegans* Research Community WormBook, doi/10.1895/wormbook.1.12.2, http://www.wormbook.org.

Hobert, O., 2016a A map of terminal regulators of neuronal identity in *Caenorhabditis elegans*. Wiley Interdiscip. Rev. Dev. Biol. 5: 474–498.

Hobert, O., 2016b Terminal selectors of neuronal identity. Essays on developmental biology. P&T 116: 455.

Huang, D. W., B. T. Sherman, and R. A. Lempicki, 2009 Systematic and integrative analysis of large gene lists using DAVID bioinformatics resources. Nat. Protoc. 4: 44–57.

Huang, M., Z. Zhou, and S. J. Elledge, 1998 The DNA replication and damage checkpoint pathways induce transcription by inhibition of the Crt1 repressor. Cell 94: 595–605.

Huang, N. N., D. E. Mootz, A. J. M. Walhout, M. Vidal, and C. P. Hunter, 2002 MEX-3 interacting proteins link cell polarity to asymmetric gene expression in *Caenorhabditis elegans*. Development 129: 747–759.

Jensen, V. L., S. Carter, A. A. W. M. Sanders, C. Li, J. Kennedy *et al.*, 2016 Whole-organism developmental expression profiling identifies RAB-28 as a novel ciliary GTPase associated with the BBSome and intraflagellar transport. PLoS Genet. 12: e1006469.

Karlsson, A. B., J. Washington, V. Dimitrova, C. Hooper, A. Shekhtman *et al.*, 2014 The role of spartin and its novel ubiquitin binding region in DALIS occurrence. Mol. Biol. Cell 25: 1355–1365.

Laurencon, A., R. Dubruille, E. Efimenko, G. Grenier, R. Bissett *et al.*, 2007 Identification of novel regulatory factor X (RFX) target genes by comparative genomics in drosophila species. Genome Biol. 8: R195.

Lubelsky, Y., N. Reuven, and Y. Shaul, 2005 Autorepression of rfx1 gene expression: functional conservation from yeast to humans in response to DNA replication arrest. Mol. Cell. Biol. 25: 10665–10673.

Mahoney, T. R., S. Luo, and M. L. Nonet, 2006 Analysis of synaptic transmission in *Caenorhabditis elegans* using an aldicarb-sensitivity assay. Nat. Protoc. 1: 1772–1777.

Meissner, T. B., Y. Liu, K. Lee, A. Li, A. Biswas *et al.*, 2012 NLRC5 cooperates with the RFX transcription factor complex to induce MHC class I gene expression. J. Immunol. 188: 4951–4958.

Mello, C. C., J. M. Kramer, D. Stinchcomb, and V. Ambros, 1991 Efficient gene transfer in *C. elegans*: extrachromosomal maintenance and integration of transforming sequences. EMBO J. 10: 3959–3970.

Milward, K., K. E. Busch, R. J. Murphy, M. de Bono, and B. Olofsson, 2011 Neuronal and molecular substrates for optimal foraging in *Caenorhabditis elegans*. Proc. Natl. Acad. Sci. USA 108: 20672–20677.

Nechipurenko, I. V., A. Olivier-Mason, A. Kazatskaya, J. Kennedy, I. G. McLachlan *et al.*, 2016 A conserved role for girdin in basal body positioning and ciliogenesis. Dev. Cell 38: 493–506.

Nelander, S., E. Larsson, E. Kristiansson, R. Mansson, O. Nerman *et al.*, 2005 Predictive screening for regulators of conserved functional gene modules (gene batteries) in mammals. BMC Genomics 6: 68.

Olmedo, M., M. Geibel, M. Artal-Sanz, and M. Merrow, 2015 A high-throughput method for the analysis of larval developmental phenotypes in *Caenorhabditis elegans*. Genetics 201: 443–448.

Pankratz, N., J. B. Wilk, J. C. Latourelle, A. L. DeStefano, C. Halter *et al.*, 2009 Genome-wide association study for susceptibility genes contributing to familial Parkinson disease. Hum. Genet. 124: 593–605.

Patel, H., H. Cross, C. Proukakis, R. Hershberger, P. Bork *et al.*, 2002 SPG20 is mutated in Troyer syndrome, an hereditary spastic paraplegia. Nat. Genet. 31: 347–348.

Pereira, L., P. Kratsios, E. Serrano-Saiz, H. Sheftel, A. E. Mayo *et al.*, 2015 A cellular and regulatory map of the cholinergic nervous system of *C. elegans*. Elife 4: e12432.

Phirke, P., E. Efimenko, S. Mohan, J. Burghoorn, F. Crona *et al.*, 2011 Transcriptional profiling of *C. elegans* DAF-19 uncovers a ciliary base-associated protein and a CDK/CCRK/LF2p-related kinase required for intraflagellar transport. Dev. Biol. 357: 235–247.

Piasecki, B. P., J. Burghoorn, and P. Swoboda, 2010 Regulatory factor X (RFX)-mediated transcriptional rewiring of ciliary genes in animals. Proc. Natl. Acad. Sci. USA 107: 12969–12974.

Piasecki, B. P., T. A. Sasani, A. T. Lessenger, N. Huth, and S. Farrell, 2017 MAPK-15 is a ciliary protein required for PKD-2 localization and male mating behavior in *Caenorhabditis elegans*. Cytoskeleton (Hoboken) 74: 390–402.

Pyke, D. A., and J. N. Thompson, 1986 Statistical-analysis of survival and removal rate experiments. Ecology 67: 240–245.

Reith, W., and B. Mach, 2001 The bare lymphocyte syndrome and the regulation of MHC expression. Annu. Rev. Immunol. 19: 331–373.

Ruaud, A., I. Katic, and J. Bessereau, 2011 Insulin/insulin-like growth factor signaling controls non-dauer developmental speed in the nematode *Caenorhabditis elegans*. Genetics 187: 337–343.

Saito, T. L., S. Hashimoto, S. G. Gu, J. J. Morton, M. Stadler *et al.*, 2013 The transcription start site landscape of *C. elegans*. Genome Res. 23: 1348–1361.

Schackwitz, W. S., T. Inoue, and J. H. Thomas, 1996 Chemosensory neurons function in parallel to mediate a pheromone response in *C. elegans*. Neuron 17: 719–728.

Schafer, J. C., C. J. Haycraft, J. H. Thomas, B. K. Yoder, and P. Swoboda, 2003 XBX-1 encodes a dynein light intermediate chain required for retrograde intraflagellar transport and cilia assembly in *Caenorhabditis elegans*. Mol. Biol. Cell 14: 2057–2070.

Schroeder, N. E., R. J. Androwski, A. Rashid, H. Lee, J. Lee *et al.*, 2013 Dauer-specific dendrite arborization in *C. elegans* is regulated by KPC-1/Furin. Curr. Biol. 23: 1527–1535.

Senti, G., and P. Swoboda, 2008 Distinct isoforms of the RFX transcription factor DAF-19 regulate ciliogenesis and maintenance of synaptic activity. Mol. Biol. Cell 19: 5517–5528.

Senti, G., M. Ezcurra, J. Löbner, W. R. Schafer, and P. Swoboda, 2009 Worms with a single functional sensory cilium generate proper neuron-specific behavioral output. Genetics 183: 595–605.

Serrano-Saiz, E., R. J. Poole, T. Felton, F. Zhang, E. D. De La Cruz *et al.*, 2013 Modular control of glutamatergic neuronal identity in *C. elegans* by distinct homeodomain proteins. Cell 155: 659–673.

Shaye, D. D., and I. Greenwald, 2011 OrthoList: a compendium of *C. elegans* genes with human orthologs. PLoS One 6: e20085.

Sieburth, D., Q. Ch'ng, M. Dybbs, M. Tavazoie, S. Kennedy *et al.*, 2005 Systematic analysis of genes required for synapse structure and function. Nature 436: 510–517.

Slos, D., W. Sudhaus, L. Stevens, W. Bert, and M. Blaxter, 2017 *Caenorhabditis monodelphis* sp. n.: defining the stem morphology and genomics of the genus *Caenorhabditis*. BMC Zoology 2: 4.

Starich, T. A., R. K. Herman, C. K. Kari, W. H. Yeh, W. S. Schackwitz *et al.*, 1995 Mutations affecting the chemosensory neurons of *Caenorhabditis elegans*. Genetics 139: 171–188.

Su, J., H. Chiang, P. Tseng, W. Tai, C. Hsu *et al.*, 2014 RFX-1-dependent activation of SHP-1 inhibits STAT3 signaling in hepatocellular carcinoma cells. Carcinogenesis 35: 2807–2814.

Sulston, J. E., E. Schierenberg, J. G. White, and J. N. Thomson, 1983 The embryonic cell lineage of the nematode *Caenorhabditis elegans*. Dev. Biol. 100: 64–119.

Swoboda, P., H. T. Adler, and J. H. Thomas, 2000 The RFX-type transcription factor DAF-19 regulates sensory neuron cilium formation in *C. elegans*. Mol. Cell 5: 411–421.

Tammimies, K., A. Bieder, G. Lauter, D. Sugiaman-Trapman, R. Torchet *et al.*, 2016 Ciliary dyslexia candidate genes DYX1C1 and DCDC2 are regulated by regulatory factor X (RFX) transcription factors through X-box promoter motifs. FASEB J. 30: 3578–3587.

Truong, T., Z. A. Karlinski, C. O'Hara, M. Cabe, H. Kim *et al.*, 2015 Oxidative stress in *Caenorhabditis elegans*: protective effects of spartin. PLoS One 10: e0130455.

Tusher, V. G., R. Tibshirani, and G. Chu, 2001 Significance analysis of microarrays applied to the ionizing radiation response. Proc. Natl. Acad. Sci. USA 98: 5116–5121.

Vayndorf, E. M., C. Scerbak, S. Hunter, J. R. Neuswanger, M. Toth *et al.*, 2016 Morphological remodeling of *C. elegans* neurons during aging is modified by compromised protein homeostasis. NPJ Aging Mech. Dis. 2: 16001.

Wang, J., H. T. Schwartz, and M. M. Barr, 2010 Functional specialization of sensory cilia by an RFX transcription factor isoform. Genetics 186: 1295–1307.

Wu, Y., J. F. Zhang, T. Xu, L. Xu, J. Qiao *et al.*, 2016 Identification of therapeutic targets for childhood severe asthmatics with DNA microarray. Allergol. Immunopathol. (Madr.) 44: 76–82.

Xie, Y., M. Moussaif, S. Choi, L. Xu, and J. Y. Sze, 2013 RFX transcription factor DAF-19 regulates 5-HT and innate immune responses to pathogenic bacteria in *Caenorhabditis elegans*. PLoS Genet. 9: e1003324.

Communicating editor: C. Kaplan